Published in final edited form as:
J Neurochem. 2012 August ; 122(3): 568–581. doi:10.1111/j.1471-4159.2012.07811.x.

Subcellular localization of Regulator of G protein Signaling RGS7 complex in neurons and transfected cells

Evangelos Liapis, **Simone Sandiford**, **Qiang Wang**, **Gabriel Gaidosh**, **Dario Motti**, **Konstantin Levay**, and **Vladlen Z. Slepak***
University of Miami Miller School of Medicine, Department of Molecular and Cellular Pharmacology

Abstract

The R7 family of regulators of G protein signaling (RGS) is involved in many functions of the nervous system. This family includes RGS6, RGS7, RGS9, and RGS11 gene products and is defined by the presence of the characteristic DEP, DHEX, GGL and RGS domains. Here, we examined the subcellular localization of RGS7, the most broadly expressed R7 member. Our immunofluorescence studies of retinal and dorsal root ganglion (DRG) neurons showed that RGS7 concentrated at the plasma membrane of cell bodies, in structures resembling lamellipodia or filopodia along the processes, and at the dendritic tips. At the plasma membrane of DRG neurons, RGS7 co-localized with its known binding partners R7BP, Gαo and Gαq. More than 50% of total RGS7-specific immunofluorescence was present in the cytoplasm, primarily within numerous small puncta that did not co-localize with R7BP. No specific RGS7 or R7BP immunoreactivity was detected in the nuclei. In transfected cell lines, ectopic RGS7 had both diffuse cytosolic and punctate localization patterns. RGS7 also localized in centrosomes. Structure-function analysis showed that the punctate localization was mediated by the DEP/DHEX domains, and centrosomal localization was dependent on the DHEX domain.

Keywords

Centrosome; neurons; G proteins; R7BP; RGS protein

Introduction

G protein-coupled receptors (GPCRs) control the activity of multiple effector enzymes and ion channels thereby regulating cellular functions. The amplitude and duration of signaling through GPCR pathways is largely dependent on the rate of GTP hydrolysis by heterotrimeric G proteins. This reaction is drastically accelerated by regulators of G protein signaling (RGS), a protein family primarily known as GTPase-activating proteins (GAPs) for G protein α subunits (Berman *et al.* 1996, Watson *et al.* 1996b, Zheng *et al.* 1999, Ross & Wilkie 2000). The RGS family consists of more than 30 members that are divided into six subfamilies according to their sequence similarity (Zheng *et al.* 1999, Ross & Wilkie 2000). Members of the R7 subfamily (RGS6, 7, 9 and 11) are predominantly expressed in the nervous system (Zhang & Simonds 2000, Larminie *et al.* 2004) and are involved in sensory signaling, motor control, neuronal development, cell division, metabolism and other

*To whom correspondence should be addressed. VSlepak@med.miami.edu.

Conflict of interest
The authors declare no conflict of interest.

processes (Garzon *et al.* 2003, Cowan *et al.* 2001, Rao *et al.* 2007, Blundell *et al.* 2008, Kovoor *et al.* 2005, Hess *et al.* 2004, Wang *et al.* 2011, Anderson *et al.* 2009b, Zhang *et al.* 2011). Recent studies established that R7 family members are also expressed at a lower level in cardiac myocytes and glands (Wang *et al.* 2011, Posokhova *et al.* 2010, Yang *et al.* 2010).

In addition to the RGS domain, which is responsible for their GAP activity, all R7 family members contain a centrally located GGL (Gγ-like) domain and an N-terminal region harboring the DEP (first found in Dishevelled, Egl-10, Pleckstrin) and DHEX (DEP helical extension) domains. The GGL domain is responsible for association with Gβ5, a divergent member of the G protein β subunit family (Cabrera *et al.* 1998, Snow *et al.* 1998, Zhang & Simonds 2000, Levay *et al.* 1999). Dimerization with Gβ5 stabilizes R7 proteins by reducing their rate of degradation in cells (Witherow *et al.* 2000). Accordingly, the Gβ5 gene knockout in mice results in elimination of the entire R7 family (Chen *et al.* 2003). Gβ5 also interacts with R7 subunits via the DEP/DHEX domains (Narayanan *et al.* 2007, Cheever *et al.* 2008, Sandiford & Slepak 2009, Porter & Koelle 2010) and in contrast to the Gβ5:GGL interaction, which is permanent, the Gβ5:DEP interaction is thought to be dynamic (Narayanan *et al.* 2007).

The GAP activity of Gβ5-R7 complexes is selective for Gαi class α subunits (Hooks *et al.* 2003, Posner *et al.* 1999, Lan *et al.* 2000) and accordingly, they regulate Gαi-mediated signaling in cellular systems (Martemyanov *et al.* 2003, Masuho *et al.* 2010, Keren-Raifman *et al.* 2001, Drenan *et al.* 2005). Gβ5-R7 complexes can also regulate Gαq-mediated signaling by non-GAP mechanisms that involve direct interactions with receptors (Sandiford *et al.* 2010). In addition to G proteins and receptors, R7 family members form complexes with the membrane anchoring proteins R7BP and R9AP (Budd *et al.* 2000, Anderson *et al.* 2007, Drenan *et al.* 2005, Martemyanov *et al.* 2005, Hu & Wensel 2002, Porter & Koelle 2010). These interactions are mediated by the DEP/DHEX domains (Anderson et al. 2007, Drenan *et al.* 2005, Martemyanov *et al.* 2005). Fractionation of brain lysates showed that R7BP is localized solely to the membranes (Anderson *et al.* 2007, Song *et al.* 2006, Grabowska *et al.* 2008), but Gβ5-RGS7 is found in both membrane-associated and cytosolic fractions (Watson *et al.* 1996a, Rose *et al.* 2000, Grabowska *et al.* 2008, Witherow *et al.* 2000, Panicker *et al.* 2010, Cao *et al.* 2008). This indicates that R7 family proteins can exist as a dimer with Gβ5 and a trimer also including R7BP. Noteworthy, the knockout of R7BP in mice had little effect on membrane association of Gβ5-RGS7 (Cao *et al.* 2008, Anderson *et al.* 2009a), which is consistent with the notion that the Gβ5-RGS7 complex can bind to the membranes in the absence of R7BP (Rose *et al.* 2000).

Subcellular localization of Gβ5-R7 complexes has been a rather controversial subject. Some investigations detected RGS7 and Gβ5 not only in the membranes and cytoplasm but also in the nuclei in certain cell lines and primary neurons (Zhang *et al.* 2001, Rojkova *et al.* 2003, Panicker *et al.* 2010). Cytoplasmic, nuclear and nucleolar localization was also observed for different splice forms of RGS6 in transfected COS-7 cells (Chatterjee *et al.* 2003, Chatterjee & Fisher 2003). Other researchers did not detect R7 complexes in the nuclei (Narayanan *et al.* 2007, Witherow *et al.* 2003, Kovoor *et al.* 2005, Song *et al.* 2006). In this paper we investigate the subcellular localization of RGS7 complexes in primary neurons and in transfected cells.

Materials and Methods

Animals and tissues

Gβ5-KO mice were provided by Dr. Ching-Kang Chen (Virginia Commonwealth University, Richmond, VA, USA) and WT C57BL6 were purchased from Jackson laboratories. Breeding and propagation of these mice was done as recently described (Wang

et al. 2011). All the animal procedures were performed according to the Guidelines for the Care and Use of Laboratory Animals of the National Institutes of Health and protocols approved by the University of Miami Committee on Use and Care of Animals.

Mouse retinas were dissected, embedded in 3% agar, and sliced on a vibratome to obtain 100 μm sections as described previously (Nair *et al.* 2005). The sections were then permeabilized with a solution of 0.1% Triton X-100, incubated with primary and secondary antibodies, and imaged using confocal microscopy.

Wild type (WT) and Gβ5 knockout (KO) male mice were sacrificed by CO_2 inhalation. Dorsal root ganglia (DRG) were dissected from adult C57BL/6 mice immediately after euthanasia. DRGs were placed in a 2 ml solution of 1mg/ml collagenase (Invitrogen) and 5 mg/ml Dispase (Worthington Biochemical) dissolved in Hibernate A-Ca (BrainBits). DRGs were incubated at 37° C in this solution for 40 min on a medium speed rocker and the resulting suspension was then centrifuged for 5 min at 100 × g. The supernatant was removed, and the pellet was resuspended in 2 ml Hibernate A (BrainBits) supplemented with B27 (Invitrogen) and glutamax (Invitrogen) and gently triturated using flame-polished glass pipettes. Triturated DRGs were centrifuged for 5 min at 100 × g and the supernatant was discarded. The pellet containing dissociated neurons was resuspended in Neurobasal-A (Invitrogen) culture media supplemented with Glutamax, B27, 0.05 μg/ml NGF (Invitrogen) and 10 μg/ml gentamycin (Invitrogen). Neurons were then plated at the density of 500-2000 cells/cm^2 on 18 mm glass coverslips pre-coated with 100 μg/ml poly-D-lysine (Sigma-Aldrich) and 10 μg/ml laminin (Sigma-Aldrich). The cells were allowed to grow in the CO_2 incubator at 37° C in a humidified atmosphere before fixing and staining.

Reagents and Antibodies

Unless stated otherwise, all chemicals were obtained from Sigma. The rabbit RGS7 antibody was described previously (Witherow *et al.* 2000). The goat anti-RGS7 (C-19, sc-8139), rabbit anti-Gαq (sc-393) and anti-Gαo (sc-387) antibodies were purchased from Santa Cruz Biotechnology, Santa Cruz, CA, USA. The rabbit antibody against R7BP (Grabowska *et al.* 2008) was provided by Dr. K. Blumer (Washington University). Anti-γ-tubulin (ab11316) was from Abcam, MA, USA and anti-β-III tubulin from TUJ, Aves Labs, OR, USA. The mouse anti-GFP antibody was from Covance. Secondary antibodies were obtained from Jackson laboratories, Invitrogen or Li-cor.

Constructs for expression in mammalian cells

Full-length— *YFP-RGS7* Bovine RGS7 cDNA was subcloned into the pEYFP-C1 vector (Clonetech) as described previously (Witherow *et al.* 2003).

Deletion mutants of RGS7; RGS7-ΔDEP—The construct lacking the DEP domain (amino acids 34-125) was described previously (Narayanan *et al.* 2007). *RGS7-ΔGGL:* The deletion of amino acids 249-305 (GGL domain) was generated earlier using PCR mutagenesis, as described in (Levay *et al.* 1999). *YFP-RGS7$^{1-248}$:* The construct lacking the GGL and RGS domains and encoding the N-terminal 248 amino acids of RGS7 was described earlier (Narayanan *et al.* 2007). The YFP-fusion construct that lacks the RGS domain and the C-terminus of RGS7 (*YFP-RGS7-ΔRGS*) was previously described (Sandiford & Slepak 2009).

YFP-DEP—Nucleotides 1-372 corresponding to amino acids 1-124 of RGS7 were PCR amplified from full-length bovine RGS7 and cloned into the pEYFP-C1 vector at the BglII and HindIII sites, as previously described (Sandiford & Slepak 2009).

YFP-DHEX—Nucleotides 372-744 corresponding to amino acids 124-248 of RGS7 (DHEX domain plus linker) were PCR amplified from full length bovine RGS7 and cloned into the pEYFP-C1 vector at the BglII and HindIII sites.

Western blot analysis

Protein samples were resolved by SDS PAGE, transferred to nitrocellulose membranes and probed with antibodies as described previously (Sandiford & Slepak 2009). The immune complexes were detected with the Odyssey florescence imaging system (Li-cor).

Mammalian cell culture and transfection

CHO-K1 cells were purchased from ATCC and cultured in F-12K Nutrient Mixture (Kaighn's modification) with 10% FBS and penicillin/streptomycin in 12-well plates at a density of 2×10^5 cells per well 16-24 h prior to transfection. Transfection was carried out using Transit LT1 transfection reagent (Mirus Bio) according to the manufacturer's instructions. 1 μg of total plasmid DNA was mixed with 2.5 μl Transit-LT1 reagent in 100 μl of OPTI-MEM Media (Invitrogen) and the mixture was incubated at room temperature for 20 min. The ratio of RGS7 to Gβ5 plasmid DNA was maintained at 5:1, with a total of 1 μg of DNA per well. LacZ DNA was used to ensure that the total DNA per plate remained constant. The Transit-LT1 reagent-DNA complex was added drop-wise to the wells, and the cells were incubated for 4-24 h, according to the requirements of each experiment.

Tissue preparation and cell fractionation

For analysis of DRG, 25-30 ganglia were dissected, homogenized using a motorized plastic tissue grinder in homogenization buffer (10 mM Tris pH 8, 1 mM EDTA, 1 mM DTT), and sonicated for 5 s using a Microson Ultrasonic Cell Disruptor (Qsonica, Newtown, CT, USA). The final concentration of total protein in the homogenate was 5 mg/ml. All the procedures were carried out on ice and in the presence of a protease inhibitor cocktail (complete EDTA-free, Roche). DRG homogenates were centrifuged at 100,000 × g for 1 h at 40C. The supernatant was saved as the soluble fraction and the pellet was resuspended to the original volume in the homogenization buffer. The final cytosolic and crude membrane fractions were dissolved in 2% SDS for electrophoresis.

Immunocytochemistry

DRG neurons were fixed with 4% paraformaldehyde and 4% sucrose in 1× PBS for 30 min at room temperature. After five washes in PBS, cells were permeabilized and pre-blocked in 0.03% Triton X-100 and 5% normal donkey serum (Jackson laboratories) in PBS for 1 h at room temperature. The blocking buffer was then aspirated and the coverslips were incubated with the primary antibodies diluted in 100 μl of the same buffer per 18 mm coverslip for 1 h at room temperature. The dilutions were 1:100 for anti-RGS7, 1:250 for R7BP, 1:500 for β-III tubulin, 1:250 for Gαq, 1:250 for Gαo and 1:250 for γ-tubulin antibodies. Following five washes in PBS, the coverslips were incubated with donkey-raised secondary antibodies diluted in blocking buffer for 1 h at room temperature protected from bright light. Secondary antibody dilutions were 1:1000 for Alexa 488 anti-rabbit, 1:400 Cy-3 anti-rabbit, 1:1000 Alexa 488 anti-goat, 1:1000 Alexa 488 anti-chicken, 1:500 Alexa 546 anti-chicken. The coverslips were then washed five times in PBS and mounted on superfrost glass slides using Prolong Gold with or without DAPI (Invitrogen). The slides were sealed and kept at 4° C.

Transfected CHO-K1 cells grown on 18 mm glass coverslips were fixed in 4% paraformaldehyde and 4% sucrose in 1× PBS at 4° C for 10 min. In experiments using the γ-tubulin antibody, cells were fixed in 4% paraformaldehyde for 2 min at room temperature, followed by ice-cold methanol at −20° C for 3 min. Fixation was quenched by washing in

0.1 M glycine in PBS for 5 min and washed five times in PBS. Cells were permeabilized with 0.25% Triton X-100 in PBS for 5 min, followed by 2 washes in PBS, and then blocked by 10% BSA in PBS for 30 min at room temperature. Primary antibodies were diluted in 3% BSA in PBS and applied to the coverslips for 1 h at room temperature. After four 5 min washes in PBS, coverslips were incubated with secondary antibodies diluted in 3% BSA for 45 min. Following five washes in PBS, the coverslips were mounted and stored as described above.

Microscopy

Images were acquired on a Leica TCS SP5 confocal microscope (Leica Microsystems GmbH, Manheim, Germany) using a 20× air (0.7-numerical aperture) and a 63× oil immersion objective (1.4-numerical aperture), typically at Airy 0.8 (0.6 μm optical sections). The highest fluorescent signals were acquired close to the maximum intensity limit and saturation was avoided by utilizing the LUT (Look-Up Table) overlay of the software. All parameters used in the acquisition step (output laser power, acquisition mode, pinhole diameter, detector gain, amplifier offset) were standardized for all samples analyzed. Images were acquired with a sequential scan to minimize crosstalk of secondary antibodies or fluorochromes. Image analysis and quantification were performed using the Leica LAS AF software. Three-dimensional reconstructions were created with the Volocity 3D Image Analysis Software, ver. 6.0 (PerkinElmer) and the Leica LAS AF software. Some of the images were acquired by a wide-field Nikon Eclipse TE2000 fluorescence microscope, using a 60× oil objective.

Image analysis and quantification

Primary DRG neurons from WT and Gβ5 KO (KO) mice were cultured and stained under identical conditions. For RGS7, background signal was measured as the mean fluorescence intensity in a region of interest (ROI) spanning the entire somata of 8-12 randomly selected KO neurons. The resulting mean value was subtracted from the signal obtained in WT neurons stained with both primary and secondary antibodies. For quantification of R7BP, the background was determined as a mean fluorescence value obtained with the secondary antibody alone; this value was then subtracted from the total immunofluorescent signal acquired with the anti-R7BP antibody.

2D analysis—A mid-plane optical section through the DRG nucleus was acquired for each neuron. The optical section was divided into plasma membrane, cytoplasm and nucleus by manually drawing a ROI around each compartment. The nuclei were outlined using DAPI staining. To measure the total amount of immunofluorescent signal within each cellular compartment, integrated pixel intensity values were determined for each ROI, using the Leica LAS AF software.

3D analysis—The measurement of fluorescence intensity for the entire volume of DRG somata was performed using a stack of ten optical sections collected for each neuron. The total pixel intensity values per ROI were counted for each optical slice and summed up to produce the total fluorescence distribution for each compartment across the 3D volume of the soma.

Statistical analysis

Quantitative analysis of the microscopic data was performed to determine the mean and standard deviation of such parameters as fluorescence intensity and percentage of cells of certain phenotype using Microsoft Excel, as described in the corresponding Figure legends.

Results

Localization of RGS7 in the retina

Consistent with earlier reports (Witherow *et al.* 2000, Cao *et al.* 2008, Mojumder *et al.* 2009), immunostaining of mouse retinal sections showed that RGS7 was absent in photoreceptors but present in neurons of the inner retina (Fig. 1). Two different anti-RGS7 antibodies (from rabbit and goat) showed nearly identical localization patterns. As expected, neither RGS7 nor R7BP were present in the retinas of the Gβ5 knockout mice, confirming the specificity of immunostaining. In agreement with previous studies (Rao *et al.* 2007, Morgans *et al.* 2007, Chen *et al.* 2010, Cao *et al.* 2008), RGS7 was abundant in the dendritic tips of bipolar cells and within two distinct layers of the inner plexiform layer (IPL) (Fig. 1b). R7BP was primarily localized in the IPL, where it was present in the somata and processes of neurons morphologically resembling amacrine cells (Song *et al.* 2007, Voigt 1986), (Fig. 1b, Supplementary video 1). Neither RGS7 nor R7BP were present in the nuclei of retinal neurons.

We noticed that in the cell bodies and processes of retinal neurons, RGS7 immunoreactivity localized to distinct puncta (Fig. 1b), and the R7BP antibody revealed a similar pattern. The small size of the retinal neurons made it difficult to determine whether the granules were associated with the plasma membranes or were localized within the cytoplasm.

Localization of RGS7 in DRG neurons

To better distinguish between membrane and cytoplasmic localization of RGS7, we investigated DRG neurons, which have very large somata. In contrast to β-III tubulin, which was evenly distributed along the neurite length, RGS7 mostly concentrated in the soma and tips of neurites (Fig. 2a). A relatively small amount of RGS7 and R7BP was also present along the neurites, where RGS7- and R7BP-positive puncta were found in structures resembling filopodia and lamellipodia (Fig. 2b, Supplementary video 2). In neurite growth cones, these puncta extend beyond β-III tubulin staining (Fig. 2b). In the cell bodies, RGS7 and R7BP were absent from the nuclei and present both in the plasma membrane and in numerous puncta scattered throughout the cytoplasm (Figs. 2-4, Supplementary video 3).

Next, we addressed the question of whether RGS7 co-localizes with R7BP and Gα subunits. For double staining, we used the available rabbit anti-R7BP, Gαo and Gαq antibodies, together with the goat anti-RGS7 antibody. As expected, a control co-staining experiment with the goat and rabbit anti-RGS7 antibodies resulted in almost complete overlap of the two fluorescence signals within the entire cell (Fig. 3a). The overall immunostaining patterns of R7BP and RGS7 were also similar in the plasma membrane of the cell body (Fig. 3b). However, RGS7 and R7BP puncta did not co-localize in the cytoplasm and only partial co-localization was observed along the neurites (Fig. 3b, lower panels). Furthermore, R7BP was relatively more abundant at the plasma membrane than in the cytoplasmic puncta. As expected, Gαo and Gαq primarily localized at the plasma membrane, and their presence in the cytosol was much less prominent compared to RGS7. Gαo and Gαq co-localized extensively with RGS7 in both the plasma membrane and the neurite tips (Figs. 3c). We did not detect any significant RGS7, R7BP or Gα immunoreactivity in the nuclei.

Quantitative analysis of RGS7 distribution in separate cell compartments required measuring specific RGS7 immunofluorescence signal (Fig. 4). First, we used DRG neurons from Gβ5 KO mice to determine the background produced with anti-RGS7 antibodies (Figs. 4a, b). The KO neurons had no signal in the plasma membrane, but the cytoplasm showed diffuse fluorescence and contained puncta, which, however, were much less numerous and bright than in the WT neurons stained under the same conditions. The average value of the signal from KO neurons was considered non-specific staining. After subtraction of this

background from images of WT neurons, the diffuse RGS7 signal from the cytoplasm or nuclei was nearly completely eliminated, whereas the bulk of immunostaining was still present on the plasma membrane and in the cytoplasmic puncta. At the same time, fractionation of the DRG lysates showed that a significant portion of RGS7 was present in the soluble fraction (Fig. 4e).

To measure the relative abundance of RGS7 in subcellular compartments, we acquired images of 10 evenly spaced optical slices for each analyzed DRG neuron, and quantified the specific RGS7 immunofluorescence in ROIs corresponding to the plasma membrane, cytoplasm and nucleus (Fig. 4c). The sum of fluorescence intensity within these ROIs throughout the Z-stack represented the integrated amounts of RGS7 in the entire volume of a particular compartment. The results (Fig. 4d) show that distribution of RGS7 is almost equal between the plasma membrane and cytoplasm, with about 5% more in the latter. Analysis of R7BP by the same approach showed that there was approximately twice as much R7BP present on the plasma membrane compared to the cytoplasm. Less than ~0.5% of RGS7 or R7BP is detected in the nucleus, a value that is statistically insignificant.

Analysis of RGS7 in transfected cells

To test whether the ectopically expressed RGS7 complex can recapitulate the localization of the native protein, we transiently expressed the YFP-RGS7 fusion construct in CHO-K1 cells. In the course of these studies we noticed that the phenotypic distribution of RGS7 depended on the time passed after transfection (Figs. 5, 6, S1). Four-five hours post-transfection, YFP-RGS7 was distributed homogenously throughout the cytoplasm of approximately 40% of cells that displayed fluorescence (Figs. 5a, 5d, S1). At this time point, RGS7 is not detectable by immunoblotting, because only a small fraction of transfected cells begin expression (Fig. 5b). The punctate pattern resembling the one observed in neurons also began to appear 4 h post-transfection and could be discerned in about 60% of cells (Figs. 5a, d). By 8 h, the fractions of diffused and punctate were slightly reduced (32% and 55% respectively, Figs. 5a, d), and cells containing large granular aggregates began to appear. The proportion of cells with this new phenotype grew progressively and by 24 h, more than 40% of cells contained granules; about 30% displayed a punctate pattern and another 30% a diffuse distribution (Fig. 5d). Co-transfection with Gβ5 had no effect on the expression levels (Fig. 5c) or localization pattern (data not shown) of YFP-RGS7. A similar localization was observed when we transfected cells with RGS7 fused to Dendra2, a monomeric fluorescent protein derived from a coral (Chudakov *et al.* 2007) (Fig. S1). Indirect immunofluorescence staining of cells transfected with untagged or FLAG-tagged RGS7 constructs visualized with anti-RGS7 and anti-FLAG antibodies also produced similar localization patterns in transfected CHO-K1, COS-7 and HEK293T cells (data not shown).

We noticed that YFP-RGS7 localizes to a single bright spot near the nuclear membrane. This spot resembled the centrosome. Indeed, co-staining of transfected CHO-K1 cells with antibodies against the centrosomal marker γ-tubulin demonstrated co-localization of YFP-RGS7 with γ-tubulin (Figs. 5a, 6c). Importantly, this co-localization was observed in nearly 100% of cells expressing RGS7 constructs, regardless of the presence of Gβ5. In cells containing multiple RGS7-positive puncta, only a single punctum co-localized with γ-tubulin (Figs. 5a, 6c, S1). Notably, centrosomal staining by the anti-γ-tubulin antibody was undetectable in the majority of cells showing large RGS7 aggregates (Figs. 5a, S1), possibly as a result of cellular stress associated with overexpression.

To investigate the role of specific structural elements of RGS7 in its localization, we examined a panel of RGS7 deletion mutants (Figs. 6a). As shown in Fig. 6c, mutants lacking the GGL and RGS domains (RGS7-ΔGGL and YFP-RGS7-ΔRGS) localized similarly to

the full-length RGS7, suggesting that neither GGL nor RGS domains are required for the punctate distribution of Gβ5-RGS7. In contrast, deletion of the DEP domain (RGS7-ΔDEP) resulted in an even distribution, indicating that the DEP domain is required for targeting to the puncta. However, the YFP-DEP fusion protein was evenly distributed across the cells, including in the nuclei (Fig. 6c). This suggested that the DEP domain alone is necessary but not sufficient for punctate distribution. The larger RGS7 construct containing DEP, DHEX and the linker sequence (YFP-RGS7$^{1-248}$) localized similarly to the full length RGS7. Thus, both DEP and DHEX domains are required for the localization of Gβ5-RGS7 to the puncta. In agreement with previous reports (Drenan *et al*. 2005, Narayanan *et al*. 2007, Drenan *et al.* 2006, Song *et al*. 2006) Gβ5-RGS7 was recruited to the plasma membrane of HEK293T cells upon co-transfection with R7BP, and the localization of Gβ5-RGS7 in cytosolic granules was abolished (data not shown). Deletion of the DEP, RGS or GGL domains did not affect the centrosomal localization of RGS7 (Fig. 6c), but a mutant lacking the DHEX domain (Fig. 6c, YFP-DEP) did not co-localize with the centrosome. To test if the DHEX domain was sufficient for centrosomal targeting of RGS7 we transfected CHO-K1 cells with a construct containing amino acids 124-248 of RGS7 (YFP-DHEX). YFP-DHEX was concentrated at the centrosome of essentially all cells expressing this construct (Fig. 6c, Fig S2), but it was also present at a lower concentration in the cytoplasm and nucleus. After longer transfection periods, YFP-DHEX formed large aggregates, while the small punctate localization pattern was not observed (Fig. S2).

Discussion

In this study we analyzed the subcellular localization of RGS7 in neurons and found that a significant fraction is present in cytoplasmic puncta. Since the hallmark function of RGS proteins is their GAP activity toward G proteins, one can expect them to localize at the plasma membrane. However, previous studies using fluorescence microscopy detected many RGS proteins not only in plasma membranes, but also in other cell compartments (Chatterjee & Fisher 2000, Burgon *et al.* 2001, Kim *et al.* 1999, Zhang *et al*. 2001, Rojkova *et al*. 2003, Panicker *et al*. 2010, Chatterjee *et al*. 2003, Chatterjee & Fisher 2003). Here, we did not detect RGS7 in the nuclei of DRG or retinal neurons or in transfected model cell lines.

The uniquely large dimensions of DRG neurons provided us with an effective resolution between cell compartments and allowed quantitative analysis of immunofluorescence data. The overall “patchy” pattern of RGS7 (Figs. 1-4) and its localization in structures resembling filopodia and lamellipodia was reminiscent of the distribution of RGS9-2 in striatal neurons (Song *et al*. 2006, Anderson *et al*. 2007, Mancuso *et al*., Cao *et al*. 2008). Likewise, localization of RGS7 in growth cones of DRG neurons (Fig. 2) is consistent with the detection of RGS7 and RGS11 in dendritic tips of retinal bipolar cells (Rao *et al*. 2007, Morgans *et al*. 2007). However, our data demonstrate for the first time that large quantities of RGS7 are present in cytoplasmic granules of neuronal cell somata (Fig. 4).

As expected, endogenous RGS7 co-localizes with R7BP and Gα subunits Gαo and Gαq at the plasma membrane. At the same time, our data revealed a striking difference in the behavior of RGS7 *versus* its binding partners. While Gαo and Gαq were detected almost exclusively on the plasma membrane of the soma, more than 50% of RGS7 resided in cytoplasmic puncta. R7BP was also present in the cytoplasm, but the relative amount (~30%) was lower compared to RGS7. Furthermore, double staining indicated that R7BP and RGS7 do not co-localize in the cytoplasm (Fig. 3a). These findings indicate that trafficking of the RGS7 complex is independent from that of R7BP and G proteins. This notion is in agreement with earlier reports that in contrast to RGS7, 100% of native R7BP is found in the particulate fraction of brain lysates (Grabowska *et al*. 2008, Anderson *et al.*

2007, Song *et al.* 2006) and that R7BP knockout does not dramatically affect association of RGS7 with membranes (Cao *et al.* 2008). Factors such as palmitoylation and interaction with Gα subunits were shown to be involved in membrane targeting of RGS7 (Rose *et al.* 2000, Takida *et al.* 2005).

A key observation in our study is that within the cytoplasm of DRG neurons, RGS7 localizes primarily to granular structures. Importantly, some of the RGS7-positive granules are as bright as the plasma membrane and the total amount of RGS7 in these organelles is higher than in the plasma membrane (Fig. 4). Therefore, it is unlikely that RGS7 resides on cytoplasmic granules simply while “en route” to plasma membrane, and so we propose that it plays a novel role in this compartment. The cytoplasm between the puncta appears nearly devoid of RGS7 immunofluorescence, which can be interpreted as absence of soluble RGS7 (Fig. 4a, b). This is at odds with cell fractionation data showing RGS7 is present in both particulate and 100,000 × g supernatant fractions (Fig. 4e). One potential explanation to this apparent disagreement is that the cell lysis procedure causes solubilization of a certain pool of RGS7, implying distinct mechanisms of RGS7 membrane anchoring. Regardless of the explanation, it is clear that the concentration of soluble RGS7 is much lower than RGS7 associated with the granules, which raises the question if and how the cytoplasmic pool can participate in G protein signaling. It is possible that binding of the RGS7 complex to the granules is dynamic, allowing it to dissociate and diffuse across the cytoplasm as the amount of Gα-GTP reaches a certain level.

3D-reconstruction of the confocal images (Supplementary videos 1-3) indicates that RGS7 antibody-labeled puncta are not part of a continuous meshwork, but form isolated granules. The size of these granular structures was at the limit of light microscopy resolution (0.2-0.5 μm). So far, our attempts to identify these granules using antibodies against markers for endosomes and other vesicles were inconclusive, and so the nature of these structures remains unknown. Some earlier investigations described localization of endogenous RGS7 as “granular” and “perinuclear” in neurons and cell lines (Kim *et al.* 1999, Hausmann *et al.* 2002). However, those observations were not thoroughly developed, possibly because the imaging results were not as definite as our data with DRG neurons (Figs. 2-4). Prompted by the striking granular localization of native RGS7, we investigated whether ectopically expressed RGS7 could replicate this behavior. We found that the majority of RGS7-transfected cells had the punctate phenotype (Figs. 5, 6, S1). Previously, we and other investigators studied R7 proteins by transfection and described their localization as cytosolic (Drenan *et al.* 2005, Panicker *et al.* 2010, Narayanan *et al.* 2007, Witherow *et al.* 2003). Our current quantitative analysis shows that in 20-40% of cells the RGS7 signal is indeed diffuse (Fig. 5d). Apparently, this phenotype was thought as the “main” one, because biochemical fractionation showed a large fraction of RGS7 to be soluble (Witherow *et al.* 2000), and the granules were considered to be artifacts of overexpression. In this study we confirmed that 24h after transfection, the proportion of punctate and diffuse phenotypes was reduced in favor of cells containing large aggregates not observed in native cells (Fig. 5a). In contrast, small RGS7-positive puncta become visible as early as 4 h after transfection, while the expression level is still very low, which may represent the natural behavior of RGS7. The small size of these granules resembles those in neurons, but at the moment it is not known whether they represent the same organelles harboring native RGS7.

In the course of this study we made the unexpected observation that RGS7 can localize at the centrosomes of transfected cells (Figs. 5a, 6c, S1). Previously, Gαi (Cho & Kehrl 2007) RGS14 (Cho *et al.* 2005) and β-arrestin (Molla-Herman *et al.* 2008) were detected in centrosomes. Interestingly, the C. elegans *rgs-7* gene product which is homologous to human RGS3, was shown to be involved in asymmetric movements of the mitotic spindle by affecting the force on the anterior but not the posterior spindle pole (Hess *et al.* 2004).

Centrosomes were implicated in multiple aspects of neuronal development, such as neurogenesis, neuronal migration and differentiation (review, see (Higginbotham & Gleeson 2007)). Given that asymmetric cell division has a fundamental role in the differentiation of the nervous system (Hawkins & Garriga 1998, Kuo & Jan 2005) it is tempting to speculate that mammalian RGS7 complexes promote neuronal differentiation. Indeed, a recent report by Simonds and co-workers described some developmental abnormalities in the CNS of the Gβ5 KO mice (Zhang *et al.* 2011). Centrosomes are also involved in vesicular trafficking (reviewed in (Schatten 2008)) and so it is plausible that interaction of Gβ5-RGS7 with the centrosome facilitates its targeting to these vesicular structures.

Our structure-function analyses support the importance of the N-terminus in the subcellular localization of RGS7. While the role of the N-terminal DEP/DHEX domain in targeting of RGS7 to the plasma membranes via R7BP is well established (Anderson *et al.* 2007, Drenan *et al.* 2005, Martemyanov *et al.* 2005), the results presented in this paper show that DEP/DHEX is also required for RGS7 targeting to intracellular structures. Furthermore, our data indicate that the DHEX domain of RGS7 is involved in association with intracellular granules and the centrosome, which is the first function ascribed to this novel structural motif.

Supplementary Material

Refer to Web version on PubMed Central for supplementary material.

Acknowledgments

The authors thank Dr. Kendall Blumer for providing the R7BP antibody and Tatiana Slepak, Junior Tayou, Darla Karpinsky, Dr. Pantelis Tsoulfas, Dr. Hassan Al Merheby and Dr. Jessica Lerch for their expert advice and helpful discussions. This study was supported by U.S. National Institutes of Health grants GM 060019 and EY018666 (V.Z.S).

Abbreviations

DIV	days *in vitro*
DRG	Dorsal root ganglia
GAP	GTPase-activating protein
GPCR	G protein-coupled receptor
GCL	ganglion cell layer
INL	inner nuclear layer
IPL	inner plexiform layer
IS	inner segment
LUT	Look-Up Table
ONL	outer nuclear layer
OPL	outer plexiform layer
OS	Outer segment
PBS	phosphate-buffered saline
R7BP	R7 RGS binding protein
R9AP	RGS9-1 binding protein

RGS	regulator of G protein signaling
ROI	region of interest

References

Anderson GR, Lujan R, Martemyanov KA. Changes in striatal signaling induce remodeling of RGS complexes containing Gbeta5 and R7BP subunits. Mol Cell Biol. 2009a; 29:3033–3044. [PubMed: 19332565]

Anderson GR, Lujan R, Semenov A, et al. Expression and localization of RGS9-2/G 5/R7BP complex in vivo is set by dynamic control of its constitutive degradation by cellular cysteine proteases. J Neurosci. 2007; 27:14117–14127. [PubMed: 18094251]

Anderson GR, Posokhova E, Martemyanov KA. The R7 RGS protein family: multi-subunit regulators of neuronal G protein signaling. Cell Biochem Biophys. 2009b; 54:33–46. [PubMed: 19521673]

Berman DM, Wilkie TM, Gilman AG. GAIP and RGS4 are GTPase-activating proteins for the Gi subfamily of G protein alpha subunits. Cell. 1996; 86:445–452. [PubMed: 8756726]

Blundell J, Hoang CV, Potts B, Gold SJ, Powell CM. Motor coordination deficits in mice lacking RGS9. Brain Res. 2008; 1190:78–85. [PubMed: 18073128]

Budd DC, McDonald JE, Tobin AB. Phosphorylation and regulation of a Gq/11-coupled receptor by casein kinase 1alpha. J Biol Chem. 2000; 275:19667–19675. [PubMed: 10777483]

Burgon PG, Lee WL, Nixon AB, Peralta EG, Casey PJ. Phosphorylation and nuclear translocation of a regulator of G protein signaling (RGS10). J Biol Chem. 2001; 276:32828–32834. [PubMed: 11443111]

Cabrera JL, de Freitas F, Satpaev DK, Slepak VZ. Identification of the Gbeta5-RGS7 protein complex in the retina. Biochem Biophys Res Commun. 1998; 249:898–902. [PubMed: 9731233]

Cao Y, Song H, Okawa H, Sampath AP, Sokolov M, Martemyanov KA. Targeting of RGS7/Gbeta5 to the dendritic tips of ON-bipolar cells is independent of its association with membrane anchor R7BP. J Neurosci. 2008; 28:10443–10449. [PubMed: 18842904]

Chatterjee TK, Fisher RA. Cytoplasmic, nuclear, and golgi localization of RGS proteins. Evidence for N-terminal and RGS domain sequences as intracellular targeting motifs. J Biol Chem. 2000; 275:24013–24021. [PubMed: 10791963]

Chatterjee TK, Fisher RA. Mild heat and proteotoxic stress promote unique subcellular trafficking and nucleolar accumulation of RGS6 and other RGS proteins. Role of the RGS domain in stress-induced trafficking of RGS proteins. J Biol Chem. 2003; 278:30272–30282. [PubMed: 12761220]

Chatterjee TK, Liu Z, Fisher RA. Human RGS6 gene structure, complex alternative splicing, and role of N terminus and G protein gamma-subunit-like (GGL) domain in subcellular localization of RGS6 splice variants. J Biol Chem. 2003; 278:30261–30271. [PubMed: 12761221]

Cheever ML, Snyder JT, Gershburg S, Siderovski DP, Harden TK, Sondek J. Crystal structure of the multifunctional Gbeta5-RGS9 complex. Nat Struct Mol Biol. 2008; 15:155–162. [PubMed: 18204463]

Chen CK, Eversole-Cire P, Zhang H, Mancino V, Chen YJ, He W, Wensel TG, Simon MI. Instability of GGL domain-containing RGS proteins in mice lacking the G protein beta-subunit Gbeta5. Proc Natl Acad Sci U S A. 2003; 100:6604–6609. [PubMed: 12738888]

Chen FS, Shim H, Morhardt D, Dallman R, Krahn E, McWhinney L, Rao A, Gold SJ, Chen CK. Functional redundancy of R7 RGS proteins in ON-bipolar cell dendrites. Invest Ophthalmol Vis Sci. 2010; 51:686–693. [PubMed: 19797210]

Cho H, Kehrl JH. Localization of Gi alpha proteins in the centrosomes and at the midbody: implication for their role in cell division. J Cell Biol. 2007; 178:245–255. [PubMed: 17635935]

Cho H, Kim DU, Kehrl JH. RGS14 is a centrosomal and nuclear cytoplasmic shuttling protein that traffics to promyelocytic leukemia nuclear bodies following heat shock. J Biol Chem. 2005; 280:805–814. [PubMed: 15520006]

Chudakov DM, Lukyanov S, Lukyanov KA. Tracking intracellular protein movements using photoswitchable fluorescent proteins PS-CFP2 and Dendra2. Nature protocols. 2007; 2:2024–2032.

Cowan CW, He W, Wensel TG. RGS proteins: lessons from the RGS9 subfamily. Prog Nucleic Acid Res Mol Biol. 2001; 65:341–359. [PubMed: 11008492]

Drenan RM, Doupnik CA, Boyle MP, Muglia LJ, Huettner JE, Linder ME, Blumer KJ. Palmitoylation regulates plasma membrane-nuclear shuttling of R7BP, a novel membrane anchor for the RGS7 family. J Cell Biol. 2005; 169:623–633. [PubMed: 15897264]

Drenan RM, Doupnik CA, Jayaraman M, Buchwalter AL, Kaltenbronn KM, Huettner JE, Linder ME, Blumer KJ. R7BP augments the function of RGS7*Gbeta5 complexes by a plasma membrane-targeting mechanism. J Biol Chem. 2006; 281:28222–28231. [PubMed: 16867977]

Garzon J, Lopez-Fando A, Sanchez-Blazquez P. The R7 subfamily of RGS proteins assists tachyphylaxis and acute tolerance at mu-opioid receptors. Neuropsychopharmacology. 2003; 28:1983–1990. [PubMed: 12902995]

Grabowska D, Jayaraman M, Kaltenbronn KM, Sandiford SL, Wang Q, Jenkins S, Slepak VZ, Smith Y, Blumer KJ. Postnatal induction and localization of R7BP, a membrane-anchoring protein for regulator of G protein signaling 7 family-Gbeta5 complexes in brain. Neuroscience. 2008; 151:969–982. [PubMed: 18248908]

Hausmann ON, Hu WH, Keren-Raifman T, Witherow DS, Wang Q, Levay K, Frydel B, V ZS, J RB. Spinal cord injury induces expression of RGS7 in microglia/macrophages in rats. Eur J Neurosci. 2002; 15:602–612. [PubMed: 11886441]

Hawkins N, Garriga G. Asymmetric cell division: from A to Z. Genes Dev. 1998; 12:3625–3638. [PubMed: 9851969]

Hess HA, Roper JC, Grill SW, Koelle MR. RGS-7 completes a receptor-independent heterotrimeric G protein cycle to asymmetrically regulate mitotic spindle positioning in C. elegans. Cell. 2004; 119:209–218. [PubMed: 15479638]

Higginbotham HR, Gleeson JG. The centrosome in neuronal development. Trends Neurosci. 2007; 30:276–283. [PubMed: 17420058]

Hooks SB, Waldo GL, Corbitt J, Bodor ET, Krumins AM, Harden TK. RGS6, RGS7, RGS9, and RGS11 stimulate GTPase activity of Gi family G-proteins with differential selectivity and maximal activity. J Biol Chem. 2003; 278:10087–10093. [PubMed: 12531899]

Hu G, Wensel TG. R9AP, a membrane anchor for the photoreceptor GTPase accelerating protein, RGS9-1. Proc Natl Acad Sci U S A. 2002; 99:9755–9760. [PubMed: 12119397]

Keren-Raifman T, Bera AK, Zveig D, Peleg S, Witherow DS, Slepak VZ, Dascal N. Expression levels of RGS7 and RGS4 proteins determine the mode of regulation of the G protein-activated K(+) channel and control regulation of RGS7 by G beta 5. FEBS Lett. 2001; 492:20–28. [PubMed: 11248230]

Kim E, Arnould T, Sellin L, Benzing T, Comella N, Kocher O, Tsiokas L, Sukhatme VP, Walz G. Interaction between RGS7 and polycystin. Proc Natl Acad Sci U S A. 1999; 96:6371–6376. [PubMed: 10339594]

Kovoor A, Seyffarth P, Ebert J, et al. D2 dopamine receptors colocalize regulator of G-protein signaling 9-2 (RGS9-2) via the RGS9 DEP domain, and RGS9 knock-out mice develop dyskinesias associated with dopamine pathways. J Neurosci. 2005; 25:2157–2165. [PubMed: 15728856]

Kuo CT, Jan YN. The hand that rocks the spindle. Nature cell biology. 2005; 7:858–859.

Lan KL, Zhong H, Nanamori M, Neubig RR. Rapid kinetics of regulator of G-protein signaling (RGS)-mediated Galphai and Galphao deactivation. Galpha specificity of RGS4 AND RGS7. J Biol Chem. 2000; 275:33497–33503. [PubMed: 10942773]

Larminie C, Murdock P, Walhin JP, Duckworth M, Blumer KJ, Scheideler MA, Garnier M. Selective expression of regulators of G-protein signaling (RGS) in the human central nervous system. Brain Res Mol Brain Res. 2004; 122:24–34. [PubMed: 14992813]

Levay K, Cabrera JL, Satpaev DK, Slepak VZ. Gbeta5 prevents the RGS7-Galphao interaction through binding to a distinct Ggamma-like domain found in RGS7 and other RGS proteins. Proc Natl Acad Sci U S A. 1999; 96:2503–2507. [PubMed: 10051672]

Mancuso JJ, Qian Y, Long C, Wu GY, Wensel TG. Distribution of RGS9-2 in neurons of the mouse striatum. J Neurochem. 2010; 112:651–661. [PubMed: 19912469]

Martemyanov KA, Hopp JA, Arshavsky VY. Specificity of G protein-RGS protein recognition is regulated by affinity adapters. Neuron. 2003; 38:857–862. [PubMed: 12818172]

Martemyanov KA, Yoo PJ, Skiba NP, Arshavsky VY. R7BP, a novel neuronal protein interacting with RGS proteins of the R7 family. J Biol Chem. 2005; 280:5133–5136. [PubMed: 15632198]

Masuho I, Celver J, Kovoor A, Martemyanov KA. Membrane anchor R9AP potentiates GTPase-accelerating protein activity of RGS11 × Gbeta5 complex and accelerates inactivation of the mGluR6-G(o) signaling. J Biol Chem. 2010; 285:4781–4787. [PubMed: 20007977]

Mojumder DK, Qian Y, Wensel TG. Two R7 regulator of G-protein signaling proteins shape retinal bipolar cell signaling. J Neurosci. 2009; 29:7753–7765. [PubMed: 19535587]

Molla-Herman A, Boularan C, Ghossoub R, et al. Targeting of beta-arrestin2 to the centrosome and primary cilium: role in cell proliferation control. PloS one. 2008; 3:e3728. [PubMed: 19008961]

Morgans CW, Wensel TG, Brown RL, Perez-Leon JA, Bearnot B, Duvoisin RM. Gbeta5-RGS complexes co-localize with mGluR6 in retinal ON-bipolar cells. Eur J Neurosci. 2007; 26:2899–2905. [PubMed: 18001285]

Nair KS, Hanson SM, Mendez A, et al. Light-dependent redistribution of arrestin in vertebrate rods is an energy-independent process governed by protein-protein interactions. Neuron. 2005; 46:555–567. [PubMed: 15944125]

Narayanan V, Sandiford SL, Wang Q, Keren-Raifman T, Levay K, Slepak VZ. Intramolecular interaction between the DEP domain of RGS7 and the Gbeta5 subunit. Biochemistry. 2007; 46:6859–6870. [PubMed: 17511476]

Panicker LM, Zhang JH, Posokhova E, Gastinger MJ, Martemyanov KA, Simonds WF. Nuclear localization of the G protein beta 5/R7-regulator of G protein signaling protein complex is dependent on R7 binding protein. J Neurochem. 2010; 113:1101–1112. [PubMed: 20100282]

Porter MY, Koelle MR. RSBP-1 is a membrane-targeting subunit required by the Galpha(q)-specific but not the Galpha(o)-specific R7 regulator of G protein signaling in Caenorhabditis elegans. Molecular biology of the cell. 2010; 21:232–243. [PubMed: 19923320]

Posner BA, Gilman AG, Harris BA. Regulators of G protein signaling 6 and 7. Purification of complexes with gbeta5 and assessment of their effects on g protein-mediated signaling pathways. J Biol Chem. 1999; 274:31087–31093. [PubMed: 10521509]

Posokhova E, Wydeven N, Allen KL, Wickman K, Martemyanov KA. RGS6/Gss5 complex accelerates IKACh gating kinetics in atrial myocytes and modulates parasympathetic regulation of heart rate. Circ Res. 2010; 107:1350–1354. [PubMed: 20884879]

Rao A, Dallman R, Henderson S, Chen CK. Gbeta5 is required for normal light responses and morphology of retinal ON-bipolar cells. J Neurosci. 2007; 27:14199–14204. [PubMed: 18094259]

Rojkova AM, Woodard GE, Huang TC, Combs CA, Zhang JH, Simonds WF. Ggamma subunit-selective G protein beta 5 mutant defines regulators of G protein signaling protein binding requirement for nuclear localization. J Biol Chem. 2003; 278:12507–12512. [PubMed: 12551930]

Rose JJ, Taylor JB, Shi J, Cockett MI, Jones PG, Hepler JR. RGS7 is palmitoylated and exists as biochemically distinct forms. J Neurochem. 2000; 75:2103–2112. [PubMed: 11032900]

Ross EM, Wilkie TM. GTPase-activating proteins for heterotrimeric G proteins: regulators of G protein signaling (RGS) and RGS-like proteins. Annu Rev Biochem. 2000; 69:795–827. [PubMed: 10966476]

Sandiford SL, Slepak VZ. The Gbeta5-RGS7 complex selectively inhibits muscarinic M3 receptor signaling via the interaction between the third intracellular loop of the receptor and the DEP domain of RGS7. Biochemistry. 2009; 48:2282–2289. [PubMed: 19182865]

Sandiford SL, Wang Q, Levay K, Buchwald P, Slepak VZ. Molecular organization of the complex between the muscarinic M3 receptor and the regulator of G protein signaling, Gbeta(5)-RGS7. Biochemistry. 2010; 49:4998–5006. [PubMed: 20443543]

Schatten H. The mammalian centrosome and its functional significance. Histochemistry and cell biology. 2008; 129:667–686. [PubMed: 18437411]

Snow BE, Krumins AM, Brothers GM, et al. A G protein gamma subunit-like domain shared between RGS11 and other RGS proteins specifies binding to Gbeta5 subunits. Proc Natl Acad Sci U S A. 1998; 95:13307–13312. [PubMed: 9789084]

Song JH, Song H, Wensel TG, Sokolov M, Martemyanov KA. Localization and differential interaction of R7 RGS proteins with their membrane anchors R7BP and R9AP in neurons of vertebrate retina. Mol Cell Neurosci. 2007; 35:311–319. [PubMed: 17442586]

Song JH, Waataja JJ, Martemyanov KA. Subcellular targeting of RGS9-2 is controlled by multiple molecular determinants on its membrane anchor, R7BP. J Biol Chem. 2006; 281:15361–15369. [PubMed: 16574655]

Takida S, Fischer CC, Wedegaertner PB. Palmitoylation and plasma membrane targeting of RGS7 are promoted by alpha o. Mol Pharmacol. 2005; 67:132–139. [PubMed: 15496508]

Voigt T. Cholinergic amacrine cells in the rat retina. The Journal of comparative neurology. 1986; 248:19–35. [PubMed: 2424943]

Wang Q, Levay K, Chanturiya T, et al. Targeted deletion of one or two copies of the G protein beta subunit Gbeta5 gene has distinct effects on body weight and behavior in mice. The FASEB journal: official publication of the Federation of American Societies for Experimental Biology. 2011; 25:3949–3957.

Watson AJ, Aragay AM, Slepak VZ, Simon MI. A novel form of the G protein beta subunit Gbeta5 is specifically expressed in the vertebrate retina. J Biol Chem. 1996a; 271:28154–28160. [PubMed: 8910430]

Watson N, Linder ME, Druey KM, Kehrl JH, Blumer KJ. RGS family members: GTPase-activating proteins for heterotrimeric G-protein alpha-subunits. Nature. 1996b; 383:172–175. [PubMed: 8774882]

Witherow DS, Tovey SC, Wang Q, Willars GB, Slepak VZ. G beta 5.RGS7 inhibits G alpha q-mediated signaling via a direct protein-protein interaction. J Biol Chem. 2003; 278:21307–21313. [PubMed: 12670932]

Witherow DS, Wang Q, Levay K, Cabrera JL, Chen J, Willars GB, Slepak VZ. Complexes of the G protein subunit gbeta 5 with the regulators of G protein signaling RGS7 and RGS9. Characterization in native tissues and in transfected cells. J Biol Chem. 2000; 275:24872–24880. [PubMed: 10840031]

Yang J, Huang J, Maity B, et al. RGS6, a modulator of parasympathetic activation in heart. Circ Res. 2010; 107:1345–1349. [PubMed: 20864673]

Zhang JH, Barr VA, Mo Y, Rojkova AM, Liu S, Simonds WF. Nuclear localization of G protein beta 5 and regulator of G protein signaling 7 in neurons and brain. J Biol Chem. 2001; 276:10284–10289. [PubMed: 11152459]

Zhang JH, Pandey M, Seigneur EM, Panicker LM, Koo L, Schwartz OM, Chen W, Chen CK, Simonds WF. Knockout of G protein beta5 impairs brain development and causes multiple neurologic abnormalities in mice. J Neurochem. 2011; 119:544–554. [PubMed: 21883221]

Zhang JH, Simonds WF. Copurification of brain G-protein beta5 with RGS6 and RGS7. J Neurosci. 2000; 20:RC59. [PubMed: 10648734]

Zheng B, De Vries L, Gist Farquhar M. Divergence of RGS proteins: evidence for the existence of six mammalian RGS subfamilies. Trends Biochem Sci. 1999; 24:411–414. [PubMed: 10542401]

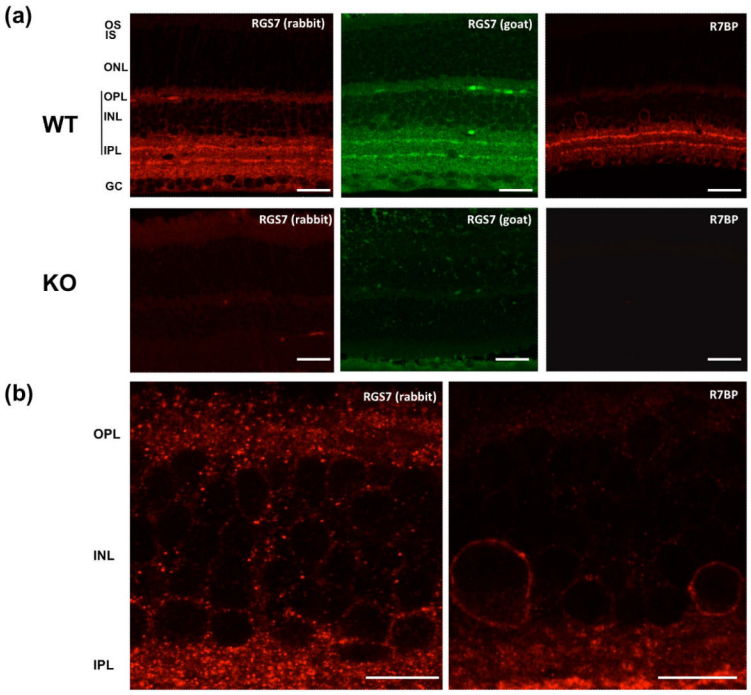

Fig. 1. Localization of RGS7 and R7BP in the mouse retina

(a) Retinal sections from wild type and Gβ5 KO mice were stained with either the rabbit anti-RGS7, goat anti-RGS7 or anti-R7BP antibodies, as described in Materials and Methods. Images were acquired on a Leica SP5 confocal microscope using a 63× oil objective. Scale bar, 25 μm. OS, Outer segment; IS, inner segment; ONL, outer nuclear layer; OPL, outer plexiform layer; INL, inner nuclear layer; IPL, inner plexiform layer; GCL, ganglion cell layer. (b) Enlargement of the OPL, INL and IPL region of a WT mouse retinal section stained with the rabbit anti-RGS7 antibody or R7BP. Scale bar, 10 μm. Data shown are representative of three independent experiments.

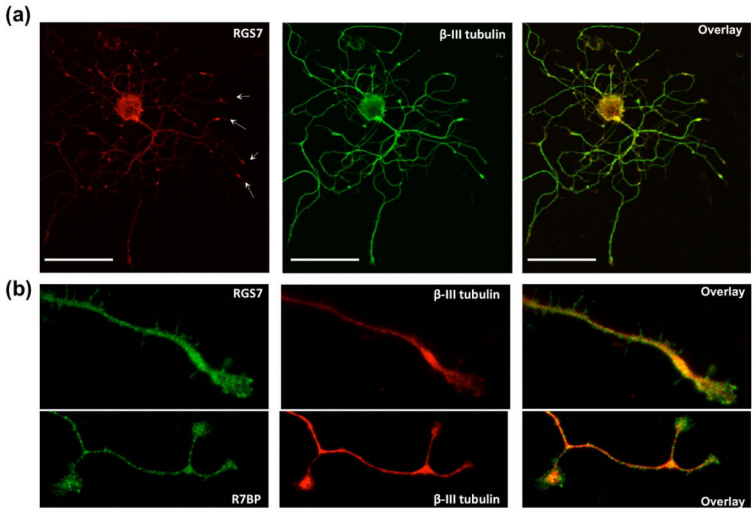

Fig. 2. Subcellular localization of RGS7 and R7BP in DRG neurons

(a) Adult mouse DRG neurons (2 DIV) were co-stained with the rabbit anti-RGS7 antibody (red) and the chicken anti-β-III tubulin antibody (green). Shown is a single optical slice acquired on a Leica TCS SP5 confocal microscope using a 20× air objective. White arrows denote neurite tips. Scale bar, 50 μm. (b) Neurite endings stained with the rabbit anti-RGS7 or anti-R7BP (green) and anti-β-III tubulin (red). Images were collected with a Nikon Eclipse TE2000 wide-field microscope using a 63× oil objective. Data shown are representative of five independent experiments.

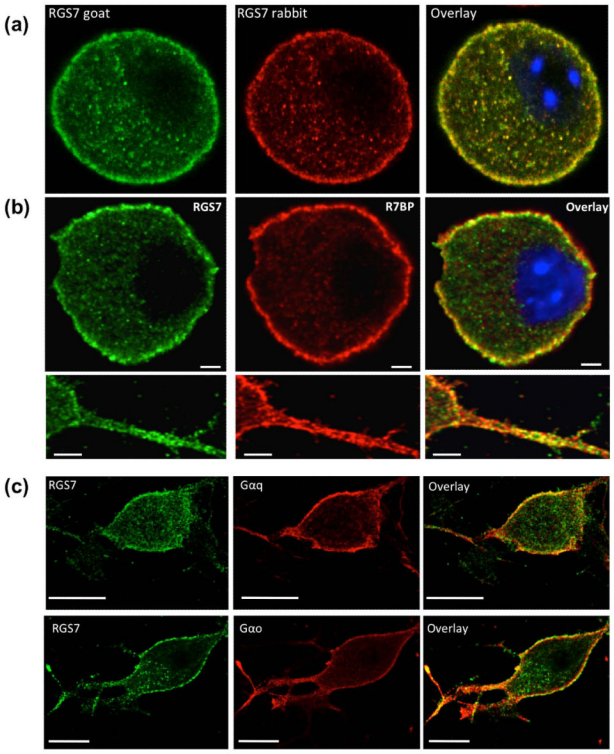

Fig. 3. Co-localization of RGS7 with R7BP, Gαq and Gαo in DRG neurons

(a) 6 DIV DRG neurons were co-stained with the goat (green) and rabbit (red) anti-RGS7 antibodies. (b) 2 DIV DRG neurons co-stained with the goat anti-RGS7 (green) and rabbit R7BP. (c) Co-staining of RGS7 with anti-Gαq and anti-Gαo antibodies (red). Images are representative single optical slices (63×) of typical DRG neuronal somata. The lower panels in (b) show the distribution of R7BP and RGS7 immunoreactivity along the neurite processes. Scale bar, 2.5 μm in (b), 25 μm in (c). Data shown are representative of five independent experiments.

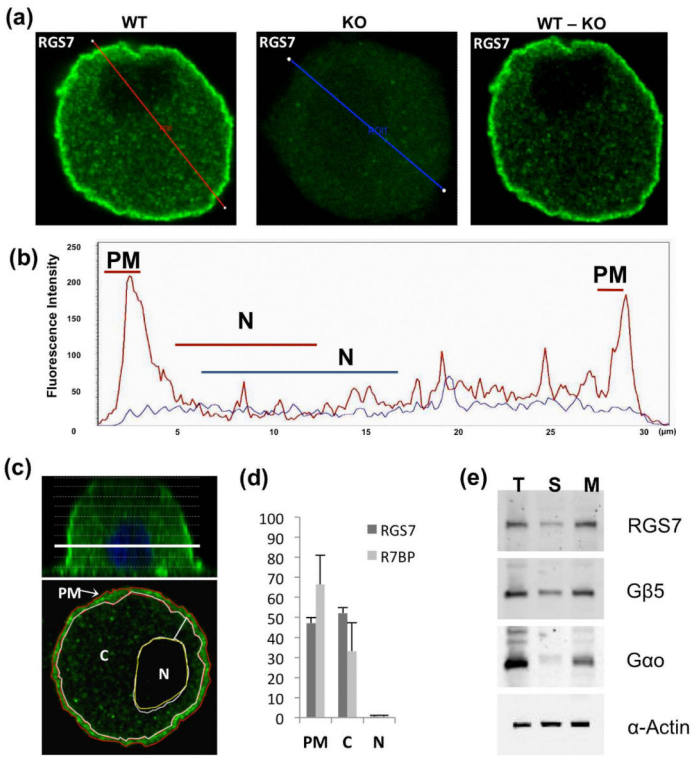

Fig. 4. Relative abundance of RGS7 and R7BP in subcellular compartments of DRG somata

(a) DRG neurons from Gβ5 KO and WT mice were stained with rabbit anti-RGS7 and anti-R7BP primary and Alexa 488 secondary antibodies. The images represent single confocal slices, acquired at Airy 0.8 (0.6 μm sections) using a 63× oil objective. The left panel shows a representative raw image of a WT DRG neuron. The central panel shows a representative KO neuron stained under identical conditions. To calculate the average background signal, the mean fluorescent intensity was determined from 12 Gβ5 KO DRG neurons (see Materials and Methods). This value was subtracted from the raw WT images; a representative processed image is shown in the right panel (WT – KO). Red and blue lines denote linear ROIs used for quantification of RGS7 signal in (b). (b) Fluorescence intensity histograms showing the distribution of RGS7 fluorescence along the soma of the WT (red trace) and KO (blue trace) DRG neurons depicted in (a). The areas corresponding to the nuclei (N) and plasma membranes (PM) are denoted above the traces. (c) Orthogonal view of a stack of optical sections collected from a single DRG neuron. The areas surrounding the plasma membrane (PM), cytoplasm (C) and the nucleus (N) were manually traced to determine the amount of RGS7 or R7BP in these selected compartments. The total fluorescence signal within the selected areas was measured using the Leica LAS AF software. The solid line denotes the position of the single optical slice shown in (a); the dashed lines indicate positions of optical slices. (d) To determine the fluorescence distribution in the entire volume of a DRG neuron, confocal stacks of ten optical slices (step size = 0.97-1.55 μm) per cell were collected. The bar graphs represent the percentage of total RGS7 or R7BP fluorescence per the indicated cell compartment. Shown are the mean +/− SD values determined for five randomly selected cells (n=5), representative from two independent experiments (e) Western blot analysis of a DRG homogenate (fractionated at 100,000 × g for 1 h at 4° C) using RGS7, Gβ5 and Gαo antibodies. Representative of two experiments. (T) Total, (S) Supernatant, (M) Membrane.

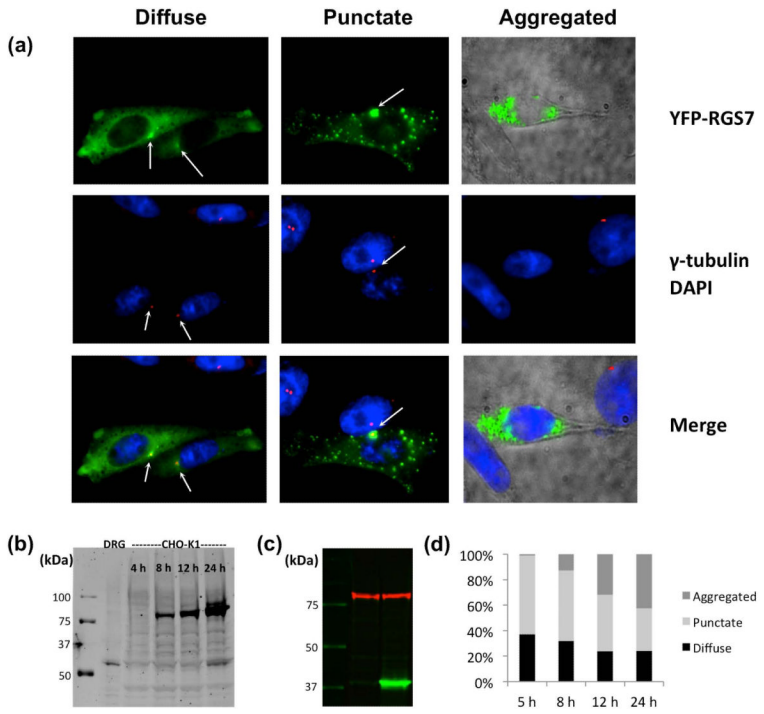

Fig. 5. Subcellular localization of YFP-RGS7 in CHO-K1 cells

(a) CHO-K1 cells were transfected with YFP-RGS7 and co-stained with an anti-γ tubulin antibody (red). Images were acquired with a Nikon Eclipse TE2000 open field microscope, using a 60× oil objective. The transfected cells were ascribed the following three phenotypes: "*Diffuse*", where the majority of YFP fluorescence was evenly distributed throughout the cytoplasm, "*Punctate*", where the fluorescence signal concentrated in small puncta and "*Aggregated*", where the signal was primarily found in larger structures often seen near the nucleus. Presented images show typical examples of these phenotypes. Arrows indicate the position of the centrosome in transfected cells. (b) Western blot comparing the expression levels of YFP-RGS7 in CHO-K1 cells transfected for 4-24 h to the level of endogenous RGS7 in a DRG homogenate. 30 μg of total protein were loaded per well; detection was performed using the rabbit anti-RGS7 antibody. (c) Cells were transiently transfected with YFP-RGS7 in the presence of LacZ or Gβ5 plasmids, harvested and analyzed by western blot, using anti-GFP (red) and anti-Gβ5 (green) antibodies. (d) CHO-K1 cells were transiently transfected with YFP-RGS7 plasmid (green) and fixed at the indicated times post-transfection, as described in Materials and Methods. The cells were counted according to the phenotype and the percentage of total number of counted cells is presented in the stacked bar graph. Cell counting was performed independently by two researchers without prior knowledge of the sample identity, and the resulting values were averaged. Shown is a representative of two independent transfection experiments. The number of counted cells was as follows: 5 h, n=162; 8 h, n=313; 12 h, n=406; 24 h, n=381.

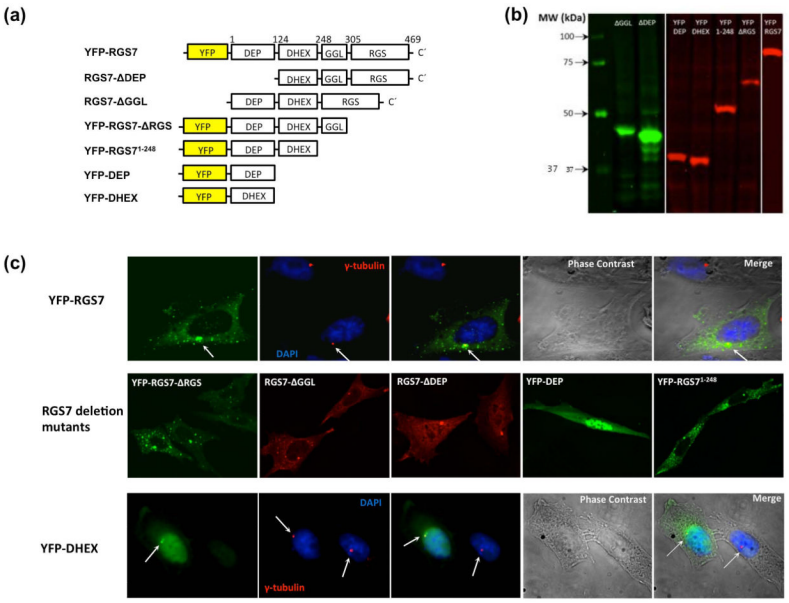

Fig. 6. Subcellular localization of RGS7 deletion mutants

(a) Schematic representation of RGS7 constructs used to transfect CHO-K1 cells. (b) Western blot analysis of the deletion mutant constructs. RGS7-ΔGGL and RGS7-ΔDEP were detected with the rabbit anti-RGS7 antibody (green) and YFP-fusion constructs with an anti-GFP antibody (red). (c) Cells were transfected with the indicated constructs for 8-12 h prior to fixation and microscopy. RGS7-ΔGGL and RGS7-ΔDEP were detected with the rabbit anti-RGS7 antibody (red) and constructs YFP-RGS7, YFP-RGS7$^{1-248}$, YFP-DEP, YFP-RGS7-ΔRGS and YFP-DHEX by direct YFP fluorescence (green). In the panels depicting YFP-RGS7 and YFP-DHEX localization, co-staining with γ-tubulin (red), DAPI (blue) and phase contrast images of the cells are also provided. Arrows indicate the centrosome. Data shown are representative of at least three independent experiments for each construct.